Hybrid metamaterials enable fast electrical modulation of freely propagating terahertz waves

Hou-Tong Chen,[1,a)] Sabarni Palit,[2] Talmage Tyler,[2] Christopher M. Bingham,[3] Joshua M. O. Zide,[4] John F. O'Hara,[1] David R. Smith,[2] Arthur C. Gossard,[4] Richard D. Averitt,[5] Willie J. Padilla,[3] Nan M. Jokerst,[2] and Antoinette J. Taylor[1]
[1]*Los Alamos National Laboratory, MPA-CINT, MS K771, Los Alamos, New Mexico 87545, USA*
[2]*Department of Electrical and Computer Engineering, Duke University, P.O. Box 90291, Durham, North Carolina 27708, USA*
[3]*Department of Physics, Boston College, 140 Commonwealth Ave., Chestnut Hill, Massachusetts 02467, USA*
[4]*Materials Department, University of California, Santa Barbara, California 93106, USA*
[5]*Department of Physics, Boston University, 590 Commonwealth Ave., Boston, Massachusetts 02215, USA*

(Received 8 July 2008; accepted 14 August 2008; published online 4 September 2008)

We demonstrate fast electrical modulation of freely propagating terahertz waves at room temperature using hybrid metamaterial devices. The devices are planar metamaterials fabricated on doped semiconductor epitaxial layers, which form hybrid metamaterial—Schottky diode structures. With an applied ac voltage bias, we show modulation of terahertz radiation at inferred frequencies over 2 MHz. The modulation speed is limited by the device depletion capacitance which may be reduced for even faster operation. © *2008 American Institute of Physics*. [DOI: 10.1063/1.2978071]

During the past two decades we have witnessed remarkable progress in terahertz science and technology, and efforts are currently underway to meet the requirements of terahertz applications. These include the development of techniques for higher power terahertz generation, more sensitive terahertz detection, and more effective control and manipulation of terahertz waves. However, the so-called terahertz gap has resulted from the general failure to translate well-developed technologies at microwave and optical frequencies to terahertz frequencies.[1] In the search for materials for terahertz applications, a class of composite artificial materials termed electromagnetic metamaterials[2–4] has emerged. Metamaterials exhibit electromagnetic properties that arise from their structure rather than solely from the materials of which they are composed. Using split-ring resonators[5] (SRRs) as typical metamaterial building blocks, the designed electromagnetic response and associated flexibility is highly desirable, particularly in the terahertz frequency range, where the resonant response dramatically enhances their interaction with terahertz radiation.[6] Recent progress in dynamically and actively switchable, frequency agile terahertz metamaterials has demonstrated their potential for practical terahertz applications.[7–11]

In this letter, we demonstrate fast electrical modulation of freely propagating terahertz waves using the hybrid terahertz metamaterial devices sketched in Fig. 1. Both are comprised of *n*-doped semiconductor material with the electrically connected metallic metamaterial SRR elements forming a Schottky diode structure. The depletion region and semiconductor conductivity, particularly near the SRR gaps, can be actively controlled with an external voltage bias between the Schottky and the Ohmic contact metallizations. In this way, the strength of the inductive-capacitive metamaterial resonance, and therefore the terahertz transmission at about 0.7 THz, is electrically modulated at room temperature with a modulation depth of 50%,[9] an order of magnitude improvement over other terahertz modulators based on semiconductor structures,[12] which often require cryogenic temperatures.[13] Despite the resonant nature, we have also found that the modulation is in fact broadband, resulting from a combination of both amplitude and phase modulation.[14] A similar approach was also employed to switch the extraordinary transmission of terahertz radiation through subwavelength metal hole arrays.[15] In this letter our terahertz transmission experiments demonstrate that the metamaterial shown in Fig. 1(a) (device A) can electrically modulate the freely propagating terahertz waves at frequencies over 100 kHz, while the improved design shown in Fig. 1(b) (device B) is able to operate in the megahertz range.

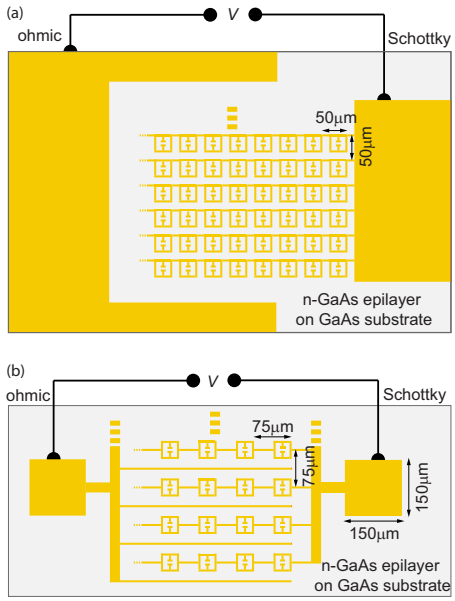

FIG. 1. (Color online) Schematic of hybrid metamaterials used as electrically driven terahertz modulators. (a) A metamaterial design (device A) having a very large Schottky electrical pad, a surrounding Ohmic contact, and a regular lattice parameter. (b) A second design (device B) with significantly smaller Schottky electrical pad, an interdigitated Ohmic contact, a larger lattice parameter, and an overall smaller active area.

a)Electronic mail: chenht@lanl.gov.

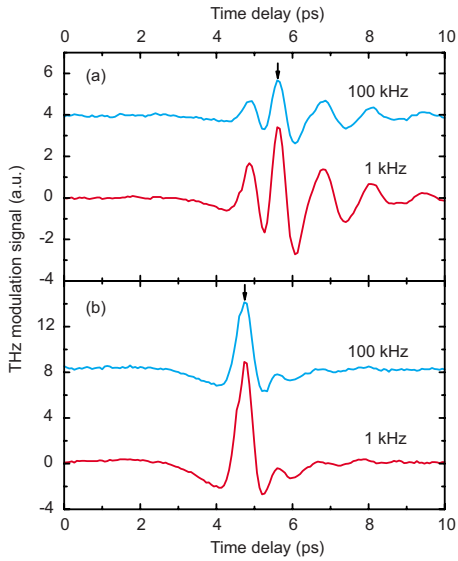

FIG. 2. (Color online) Time-domain measurements of terahertz modulation signal when applying an ac voltage alternating between 0 and 12 V (a) to device A and (b) to the photoconductive terahertz transmitter, at frequencies of 1 and 100 kHz, respectively.

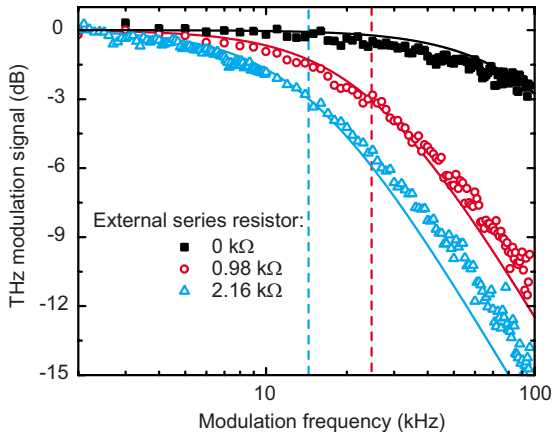

FIG. 3. (Color online) Terahertz modulation signals of device A as a function of the modulation frequency when loaded with various external series resistors. The solid curves are *RC* fits to the experimental data.

These modulation speeds significantly exceed those of other state-of-the-art electrically driven terahertz devices.[12,13,16] With further optimization, such metamaterial-based terahertz electrical modulators will be useful for real-time terahertz imaging, fast sensing and identification, and even in short-range secure terahertz communications.[17]

The metallic metamaterial SRRs were fabricated on epitaxial GaAs grown on an intrinsic GaAs substrate. The semiconductor epilayers were 1-μm-thick n-GaAs layers grown on intrinsic GaAs wafers by molecular beam epitaxy with a carrier concentration of $n_0=1.9\times10^{16}$ cm^{-3} in device A and $n_0=2\times10^{16}$ cm^{-3} in device B. The fabrication procedure of device A has already been described in detail.[9] The broad Ohmic contact in device A is replaced by an interdigitated Ohmic contact (20 nm Ge/100 nm Au/30 nm Ni/200 nm Au) in device B, and is fabricated by lift-off photolithography, followed by rapid thermal annealing at 370 °C for 1 min in a nitrogen atmosphere. Next, the Schottky metallization is deposited (10 nm Ti/15 nm Pt/200 nm Au) and defined using lift-off photolithography. The active metamaterial areas are 5×5 mm^2 in device A and 2.5×2.5 mm^2 in device B, which are either larger than or approximately equal to the diameter of the terahertz focal spot (~3 mm). Furthermore, the large Schottky electrical pad (2×5 mm^2) in device A is reduced to 150×150 μm^2 in device B, which significantly reduces the parasitic pad capacitance and improves the operational speed.

We use a photoconductive antenna based terahertz time-domain spectroscopy[18] (TDS) system to characterize the modulation of the freely propagating terahertz radiation. Terahertz transmission is recorded as a function of the frequency of an applied rectangular ac voltage bias, which alternates between 0 and −12 V ("−" means reverse bias of the Schottky diode) at frequencies varying from 1 to 100 kHz. The modulated (differential) terahertz signal is first measured in the time domain at a few different modulation frequencies, and then the peak terahertz modulation signal (indicated by the arrows in Fig. 2) is swept as a function of modulation frequency up to 100 kHz, which is the limit of our terahertz detection method. All measurements are performed at room temperature and purged with dry air to prevent terahertz absorption from the humidity.

In Fig. 2(a) we show the time-domain waveforms of the modulated terahertz signal of device A at 1 and 100 kHz, respectively. The curves have been vertically translated for clarity. As we can see, the terahertz modulation signal magnitude decreases at 100 kHz. This decrease is not only due to the metamaterial device response but also to the frequency dependence of the terahertz TDS system (including preamplifier, lock-in amplifier, etc.). We performed identical measurements modulating the bias on the photoconductive terahertz transmitter instead of the metamaterial device. The results are shown in Fig. 2(b), where we also observe a decrease in terahertz modulation magnitude at higher modulation frequencies. Consequently the following measured modulation frequency dependences of the metamaterial devices are normalized to that of the terahertz TDS system.

Figure 3 reveals the terahertz modulation signal of device A as a function of the modulation frequency. The curves have been further normalized to 0 dB at low modulation frequencies. The 3 dB roll-off frequency f_c of the terahertz modulation (black solid square) is a little beyond 100 kHz. The modulation speed is limited by the device *RC* time constant, where R is the forward resistance of the Schottky diode (126 Ω in device A), and C is its depletion capacitance. Our experimental measurement system is limited to 100 kHz, but we can infer the modulation speed by loading the metamaterial device with additional series resistance, which shifts f_c to lower frequencies. This is verified by the experimental data (red open circle and blue open triangle) in Fig. 3: when the metamaterial device is loaded in series with external 0.98 and 2.16 kΩ resistors, the measured f_c are 24 and 14 kHz, respectively. The solid curves represent the fits to the experimental data using the *RC* time constant as the fitting parameter.

Reducing the device resistance and/or capacitance can result in further improvement of the operational speed of the terahertz metamaterial modulators. Device B has an interdigitated Ohmic contact, smaller metamaterial active area, larger lattice parameter, and a significantly smaller Schottky electrical pad. The interdigitated Ohmic contact (forward resistance of 100 Ω) reduces the device resistance about 20%, and the latter three modifications dramatically decrease the device capacitance. The experimental results are shown in

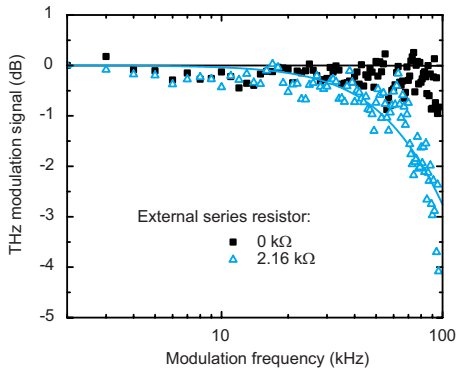

FIG. 4. (Color online) Terahertz modulation signals of device B as a function of the modulation frequency when loaded with 0 and 2.16 kΩ external series resistors. The solid curves are fits to the experimental data.

Fig. 4, with the solid curves as the *RC* fits. With the device itself, we do not observe any frequency roll-off up to the measurement limit of 100 kHz; by loading the device with a 2.16 kΩ external series resistor, it yields $f_c \sim 100$ kHz.

By measuring the frequency roll-off of the metamaterial devices in both loaded and unloaded conditions, the modulation speed can be inferred using $f_c = (2\pi RC)^{-1}$ to be ~200 kHz and ~2 MHz for devices A and B, respectively. On the other hand, the roll-off frequency of our terahertz metamaterial modulators can also be directly estimated. The output impedance of the function generator is 50 Ω and the Schottky diode forward resistances are 126 and 100 Ω, therefore $R=176$ and 150 Ω for devices A and B, respectively. The depletion capacitance C can be calculated by[19]

$$C = A\left[\frac{qN_d\varepsilon_s}{2(V_{\mathrm{bi}} - V)}\right]^{1/2}, \tag{1}$$

where $A=0.173$ and 0.012 cm^2 are the Schottky gate areas (including the electrical pad) of devices A and B, respectively, q is the electron charge, $N_d = 1.9\times10^{16}$ cm^{-3} is the approximate doping concentration of the n-GaAs substrate, $\varepsilon_s = 12.9\varepsilon_0$ is the GaAs dielectric constant where ε_0 is the vacuum permittivity,[20] $V_{\mathrm{bi}}=0.9$ V is the built-in voltage of the Schottky junction, and V is the applied voltage bias (negative values for reverse bias). During the calculations we take $V=0$, which corresponds to the largest capacitance, thereby the smallest modulation frequency of the metamaterial devices.

For device A, without any loading resistor, f_c is calculated to be 119 kHz. When loaded with 0.98 and 2.16 kΩ external series resistors, the calculated f_c are 18 and 9 kHz. For device B, f_c is calculated to be 2.1 MHz, and it is 135 kHz when loaded with a 2.16 kΩ series resistor. The calculated values are in good agreement with the experimental data, given for the use of $V=0$ in our calculations of device capacitance. Note that the nonlinear dependence of the terahertz modulation on the applied voltage as well as the leakage current under large reverse bias are not considered in the calculations, but they also affect the results and contribute to the minor deviations.

In conclusion, we have demonstrated a very fast electrically driven metamaterial terahertz modulator with high modulation depth. Based on experimental data and calculations, the modulation speed is estimated to be greater than 2 MHz. Further improvement of the modulation speed is possible if we consider the advantageous property of metamaterials that their resonant response originates from the individual inclusions. So even a small number of metamaterial elements, in which the device capacitance will be dramatically reduced, will enable modulation of freely propagating terahertz radiation, e.g., terahertz quantum cascade lasers (QCLs),[21] or guided terahertz waves,[22] with unprecedented speed. Typical terahertz QCLs have exit facets on the order of 150×10 $\mu\mathrm{m}^2$. Thus, assuming ideal scaling and utilizing the same metamaterial Schottky modulator, this implies possible terahertz QCL modulation at gigahertz speeds.

We thank Dr. Abul Azad for his support in terahertz measurements, Dr. Martin Brooke for his equivalent circuit and test discussions, and Dr. April Brown for material growths. We acknowledge support from the Los Alamos National Laboratory LDRD Program. W.J.P. acknowledges support from the Office of Naval Research Grant No. N000140710819. This work was performed, in part, at the Center for Integrated Nanotechnologies, a U.S. Department of Energy, Office of Basic Energy Sciences Nanoscale Science Research Center operated jointly by Los Alamos and Sandia National Laboratories. Los Alamos National Laboratory, an affirmative action/equal opportunity employer, is operated by Los Alamos National Security, LLC, for the National Nuclear Security Administration of the U.S. Department of Energy under Contract No. DE-AC52-06NA25396.

[1] B. Ferguson and X.-C. Zhang, Nat. Mater. **1**, 26 (2002).
[2] D. R. Smith, W. J. Padilla, D. C. Vier, S. C. Nemat-Nasser, and S. Schultz, Phys. Rev. Lett. **84**, 4184 (2000).
[3] R. A. Shelby, D. R. Smith, and S. Schultz, Science **292**, 77 (2001).
[4] T. J. Yen, W. J. Padilla, N. Fang, D. C. Vier, D. R. Smith, J. B. Pendry, D. N. Basov, and X. Zhang, Science **303**, 1494 (2004).
[5] J. B. Pendry, A. J. Holden, D. J. Robbins, and W. J. Stewart, IEEE Trans. Microwave Theory Tech. **47**, 2075 (1999).
[6] H.-T. Chen, J. F. O'Hara, A. J. Taylor, R. D. Averitt, C. Highstrete, M. Lee, and W. J. Padilla, Opt. Express **15**, 1084 (2007).
[7] W. J. Padilla, A. J. Taylor, C. Highstrete, M. Lee, and R. D. Averitt, Phys. Rev. Lett. **96**, 107401 (2006).
[8] H.-T. Chen, W. J. Padilla, J. M. O. Zide, S. R. Bank, A. C. Gossard, A. J. Taylor, and R. Averitt, Opt. Lett. **32**, 1620 (2007).
[9] H.-T. Chen, W. J. Padilla, J. M. O. Zide, A. C. Gossard, A. J. Taylor, and R. D. Averitt, Nature (London) **444**, 597 (2006).
[10] H.-T. Chen, J. F. O'Hara, A. K. Azad, A. J. Taylor, R. D. Averitt, D. B. Shrekenhamer, and W. J. Padilla, Nat. Photonics **2**, 295 (2008).
[11] T. Driscoll, S. Palit, M. M. Qazilbash, M. Brehm, F. Keilmann, B.-G. Chae, S.-J. Yun, H.-T. Kim, S. Y. Cho, N. M. Jokerst, D. R. Smith, and D. N. Basov, Appl. Phys. Lett. **93**, 024101 (2008).
[12] T. Kleine-Ostmann, P. Dawson, K. Pierz, G. Hein, and M. Koch, Appl. Phys. Lett. **84**, 3555 (2004).
[13] R. Kersting, G. Strasser, and K. Unterrainer, Electron. Lett. **36**, 1156 (2000).
[14] H.-T. Chen and A. J. Taylor (unpublished).
[15] H.-T. Chen, H. Lu, A. K. Azad, R. D. Averitt, A. C. Gossard, S. A. Trugman, J. F. O'Hara, and A. J. Taylor, Opt. Express **16**, 7641 (2008).
[16] C.-F. Hsieh, R.-P. Pan, T.-T. Tang, H.-L. Chen, and C.-L. Pan, Opt. Lett. **31**, 1112 (2006).
[17] C. Jastrow, K. Münter, R. Piesiewicz, T. Kürner, M. Koch, and T. Kleine-Ostmann, Electron. Lett. **44**, 213 (2008).
[18] J. F. O'Hara, J. M. O. Zide, A. C. Gossard, A. J. Taylor, and R. D. Averitt, Appl. Phys. Lett. **88**, 251119 (2006).
[19] M. S. Shur, *Introduction to Electronic Devices* (Wiley, New York, 1995).
[20] D. Grischkowsky, S. Keiding, M. van Exter, and Ch. Fattinger, J. Opt. Soc. Am. B **7**, 2006 (1990).
[21] R. Köhler, A. Tredicucci, F. Beltram, H. E. Beere, E. H. Linfield, A. G. Davies, D. A. Ritchie, R. C. Lotti, and F. Rossi, Nature (London) **417**, 156 (2002).
[22] R. Mendis and D. Grischkowsky, Opt. Lett. **26**, 846 (2001).